

## **Structural and antiferromagnetic properties of Sm-doped chrysene**

Xiao-Hui Wang, Guo-Hua Zhong, Jia-Xing Han, Xiao-Jia Chen, and Hai-Qing Lin

Citation: *AIP Advances* **7**, 055707 (2017); doi: 10.1063/1.4974284

View online: <http://dx.doi.org/10.1063/1.4974284>

View Table of Contents: <http://aip.scitation.org/toc/adv/7/5>

Published by the [American Institute of Physics](#)

---

---

## Structural and antiferromagnetic properties of Sm-doped chrysene

HPSTAR  
422-2017

Xiao-Hui Wang,<sup>1,2</sup> Guo-Hua Zhong,<sup>1,3,a</sup> Jia-Xing Han,<sup>1,4</sup> Xiao-Jia Chen,<sup>5</sup> and Hai-Qing Lin<sup>1</sup>

<sup>1</sup>Beijing Computational Science Research Center, Beijing 100089, China

<sup>2</sup>Department of Physics, University of Science and Technology of China, Hefei 230026, China

<sup>3</sup>Shenzhen Institutes of Advanced Technology, Chinese Academy of Sciences, Shenzhen 518055, China

<sup>4</sup>Department of Physics, Peking University, Beijing 100871, China

<sup>5</sup>Center for High Pressure Science and Technology Advanced Research, Shanghai 201203, China

(Presented 1 November 2016; received 23 September 2016; accepted 27 October 2016; published online 12 January 2017)

The experimental discovery of superconductivity was reported in Sm-doped chrysene with  $T_c \sim 5$  K, which provides vital material for exploring unique superconducting mechanism of rare-earth metal doped polycyclic aromatic hydrocarbons. Here the crystal, electronic structures and magnetic characteristics of Sm-doped chrysene have been investigated by the first-principles calculation using the generalized gradient approximation (GGA) plus  $U$  method, also including van der Waals correction. We find that Sm-doped chrysene with  $C2/c$  space group is the most stable where doped Sm atoms stay on the relative middle of chrysene molecules. This material is stabilized at antiferromagnetic ground-state with the metallic feature. The calculated spin magnetic moment of Sm atom indicates that there are two electrons transferring from Sm to chrysene molecule. Within the framework of GGA+ $U$ , the  $C-2p$  electronic states mainly contribute to the Fermi surface. Electronic correlation effects are significant to understand the superconductivity in Sm-doped chrysene. © 2017 Author(s). All article content, except where otherwise noted, is licensed under a Creative Commons Attribution (CC BY) license (<http://creativecommons.org/licenses/by/4.0/>). [<http://dx.doi.org/10.1063/1.4974284>]

### I. INTRODUCTION

The discovery of superconductivity in K-doped picene<sup>1</sup> has revitalized the research interest in polycyclic aromatic hydrocarbons (PAHs), and a large variety of PAH superconductors have been reported afterwards, such as K-doped phenanthrene, coronene and 1,2:8,9-dibenzopentacene.<sup>2-4</sup> In these class of organic superconductors, alkali metal atoms are intercalated into the interstitial space of aromatic molecules, consequently, electrons of alkali metal can be transferred to the aromatic molecules and leading to the superconductivity. Interestingly, the magnetism is not negligible in these PAH superconductors, and indeed magnetic measurements showed strong magnetic characteristics in these materials.<sup>2,3</sup> Recently a new class of PAH superconductor were reported experimentally with  $T_c \sim 5$  Kelvin for Sm-doped phenanthrene<sup>5</sup> and  $\sim 6$  Kelvin for Sm-doped chrysene.<sup>6</sup> Comparing with K-doped PAHs, it is the introduction of magnetic atoms that results in the superconductivity in Sm-doped PAHs. Thus, exploring possible magnetic interactions in Sm-doped PAHs is vital for understanding the competing magnetic-superconductive mechanism. Furthermore, the crystal structures of PAH superconductors and the positions of doped metal atoms, which are foremost to explore electronic properties and superconducting mechanism, are difficult to be determined experimentally

<sup>a</sup>Electronic mail: [gh.zhong@siat.ac.cn](mailto:gh.zhong@siat.ac.cn)



due to the sample preparation and divergence of superconducting mechanism of PAH superconductors. Therefore in this work, based on the first-principles calculation, we theoretically predicted the crystal structures, electronic properties as well as the magnetic configurations of Sm-doped chrysene ( $\text{Sm}_1\text{C}_{18}\text{H}_{12}$ ) whose precise nature is still unknown. This study is helpful for achieving a better understanding of the microstructure, magnetism and superconductivity for rare-earth-doped PAHs in the case of  $\text{Sm}_1\text{C}_{18}\text{H}_{12}$ .

## II. COMPUTATIONAL METHODS

The crystal, electronic structures and magnetic characteristics of  $\text{Sm}_1\text{C}_{18}\text{H}_{12}$  were systematically investigated by the first-principles calculation using the generalized gradient approximation (GGA)<sup>7</sup> plus on-site Coulomb energy  $U$  (namely GGA+ $U$ )<sup>8,9</sup> implemented in the VASP package,<sup>10</sup> also with van der Waals (vdW)<sup>11</sup> corrections included. The cutoff energy for plane wave basis was set as 320 eV. All the optimizations were performed using the conjugate-gradient algorithm. The Monkhorst-Pack  $k$ -point grids were generated according to the specified  $k$ -point separation  $0.04 \text{ \AA}^{-1}$  for relaxation and  $0.02 \text{ \AA}^{-1}$  for self-consistency calculation. The convergence thresholds were set as  $10^{-4}$  eV in energy and  $10^{-2}$  eV/Å in force.

Our previous studies have confirmed the GGA plus vdW correction in vdW-DF2 version<sup>11</sup> can accurately predict the crystal lattice parameters of PAHs.<sup>12</sup> Here, the first two rows of Table I list the experimental and optimized crystal lattice parameters of pristine chrysene ( $\text{C}_{18}\text{H}_{12}$ ). The lattice parameters of  $\text{C}_{18}\text{H}_{12}$  calculated by vdW-DF2 functional is in good agreement with the experimental values,<sup>13</sup> which can verify the reliability of vdW-DF2 functional. In view of the proposed experimental crystal structure,<sup>6</sup> we have investigated several crystal structures for one Sm atom doped chrysene with the most possible symmetries of  $C2/c$ ,  $P2_1$  and  $P1$  space groups. To explore the magnetism of this  $\text{Sm}_1\text{C}_{18}\text{H}_{12}$  system, we set three initial spin configurations of non-magnetic (NM), ferromagnetic (FM), and antiferromagnetic (AFM) for all the structures, respectively. The AFM configuration defined as spin antiparallel of Sm atoms between two Sm atomic layers. For local Sm-4*f* electrons, we adapted the GGA+ $U$  method to analyze the strong electronic correlation effects in the system, where  $U$  is chosen as 5.5 eV.<sup>14</sup> Of course, the influence of  $U$  parameter to electronic properties was also discussed since a different value of  $U$  was adopted in Sm-doped phenanthrene.<sup>15</sup> In addition, our calculation also included the spin-orbit coupling (SOC) to examine the contributions of spin moment and orbital moment to total magnetic moment.

## III. RESULTS AND DISCUSSION

Chrysene molecule consists of four fused benzene rings arranged in a zigzag manner.<sup>1</sup> Pristine chrysene crystallizes with the space group of  $C2/c$ , and the unit cell forms the herringbone pattern with four chrysene molecules in it. Sm is a rare-earth metal with an electron configuration  $4f^66s^2$ . Previous studies suggested that alkali metal-doped phenacene family also showed  $P2_1$  and  $P1$  symmetries,<sup>16</sup> so we focused on the magnetic configurations of  $\text{Sm}_1\text{C}_{18}\text{H}_{12}$  with  $C2/c$ ,  $P2_1$  and  $P1$  space groups.

Considering all the possible space groups and magnetic configurations of  $\text{Sm}_1\text{C}_{18}\text{H}_{12}$ , we have calculated total energies relative to the ground-state of each initial configuration. The results suggest

TABLE I. Optimized crystal lattice parameters of pristine chrysene and Sm-doped chrysene. (a) and (b) correspond to the most stable and metastable crystal structures shown in Fig. 1.

System	Method	$a$ (Å)	$b$ (Å)	$c$ (Å)	$\beta$ (°)	$V$ (Å <sup>3</sup> )
$\text{C}_{18}\text{H}_{12}$	Expt. (Ref. 13)	22.803	6.216	8.348	96.49	1175.7
	vdW-DF2	22.673	6.063	8.456	95.55	1156.8
$\text{Sm}_1\text{C}_{18}\text{H}_{12}$	Expt. (Ref. 6)	25.401	6.261	8.386	116.4	1194.6
	vdW-DF2 (a)	20.879	7.241	7.646	107.47	1102.7
	vdW-DF2 (b)	23.062	6.821	7.198	102.71	1104.5

that  $\text{Sm}_1\text{C}_{18}\text{H}_{12}$  is stabilized at the AFM ground-state with  $C2/c$  space group. The optimized crystal structure is depicted in Fig. 1(a), and Fig. 1(b) shows the relatively metastable crystal structure of  $\text{Sm}_1\text{C}_{18}\text{H}_{12}$  which is a FM stable state with the same  $C2/c$  space group. In the most stable structure, Sm atoms are seated on the bridge of 1/2-benzene ring and 3/4-benzene ring of chrysene molecules as shown in Fig. 1(a). While Sm atoms stays on the interlayer region of chrysene molecules in the metastable  $\text{Sm}_1\text{C}_{18}\text{H}_{12}$ , as shown in Fig. 1(b). The dopants moving into the interlayer region will lower the systemic stability, which had been also confirmed in K-doped picene.<sup>17</sup> The optimized crystal lattice parameters of these two structures are listed in Table I. From lattice constants, the shape of the most stable structure in theoretical prediction is far from that in experimental measurement, even if it is included in the Hubbard  $U$  correction. However, the error of volume of unit cell is only 7.7% which is in a tolerable range. From the point of view of theoretical simulation, the Sm doping reduces the volume of chrysene crystal, which is according with the situation of K-doped PAHs.

For the most stable  $\text{Sm}_1\text{C}_{18}\text{H}_{12}$ , based on GGA+ $U$  ( $U = 5.5$  eV) including the SOC effect, our calculated spin moment is about  $5.9 \mu_B$  for Sm atom, and the orbital moment of Sm is about  $-1.6 \mu_B$  with the opposite direction to the spin moment. As a result, the total magnetic moment of Sm is  $4.3 \mu_B$ . The magnetic moment of C and H atoms is very small and ignorable. It is different from that in K-doped PAHs, of which magnetic moment mainly comes from C atoms.<sup>18,19</sup> Fig. 1(c) depicts the calculated spin density of the most stable crystal structure showed in Fig. 1(a), and the blue and pink clouds correspond to the different spin directions. The expansion of spin cloud implies the magnitude of corresponding magnetic moments. One can clearly see the antiferromagnetic configurations of Sm atoms. The obvious distinction of spin cloud between C atoms and Sm atoms also indicates that AFM state is mainly induced by the antiferromagnetic states of Sm atoms, instead of C atoms which applies to the situation of K-doped PAHs. Analyzing the magnetism of Sm, we found that the calculated orbital moment ( $1.6 \mu_B$ ) in doped crystal is less than that of isolated atom ( $\sim 3.4 \mu_B$ ). The reason is mainly from the crystal field effect interacted by aromatic molecules. In addition, we found that the spin moment of Sm in doped chrysene is  $5.9 \mu_B$ , which indicates that Sm ion is at high-spin state with six  $4f$  electrons occupying the spin-up channels. Combining the calculated local magnetic moment of Sm atom with its electron configuration mentioned above, we determine that two electrons are transferred from each Sm atom to chrysene molecules, and Sm ion behaves as the  $\text{Sm}^{2+}$  valence

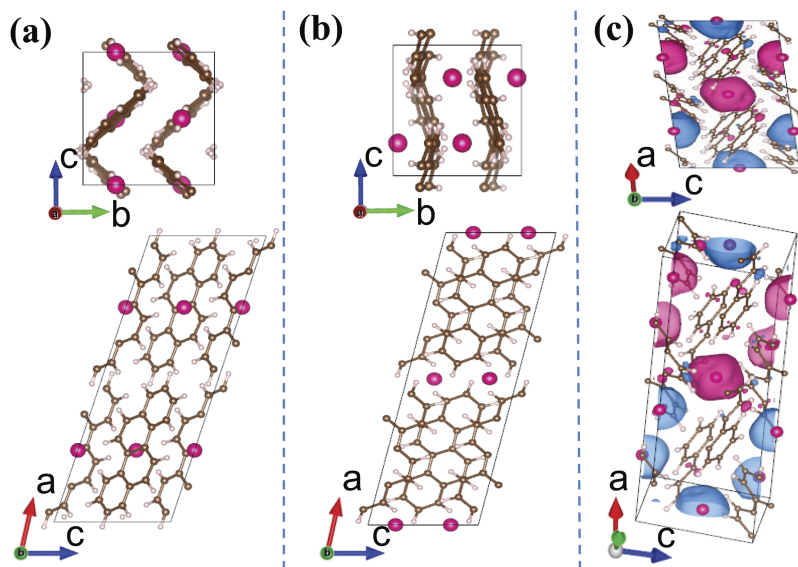


FIG. 1. Crystal structures and spin density distributions of  $\text{Sm}_1\text{C}_{18}\text{H}_{12}$ . Pink spheres represent Sm atoms. Top panels display the side view and bottom panels display the top views direction. (a) and (b) respectively corresponds to the most stable and metastable crystal structures of  $\text{Sm}_1\text{C}_{18}\text{H}_{12}$ . (c) depicts the calculated spin density of the most stable crystal structure showed in (a). The different colours of spin density in (c) represent the different spin directions.

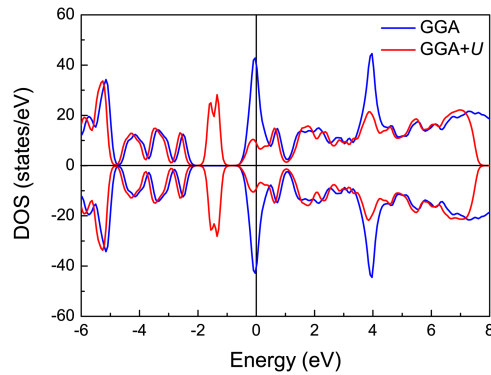


FIG. 2. Calculated total DOS of the most stable  $\text{Sm}_1\text{C}_{18}\text{H}_{12}$ , based on GGA and GGA+ $U$  method, respectively. Zero energy denotes the Fermi level.

state. The transfer of two electrons in  $\text{Sm}_1\text{C}_{18}\text{H}_{12}$  is different from those tripotassium-doped picene and phenanthrene.<sup>1,2</sup>

Fig. 2 shows spin polarized density of states (DOS) of the most stable  $\text{Sm}_1\text{C}_{18}\text{H}_{12}$  with AFM ground-state. The electrons of Sm atoms are transferred to chrysene molecules, leading the system to form a metallic state, which can be obtained by both GGA and GGA+ $U$  ( $U = 5.5$  eV) calculations. From the GGA result, there is a sharp peak localized at the Fermi level, and the electronic states at the Fermi level mainly contributed by Sm-4*f*. However, compared GGA+ $U$  with GGA treatment, the electronic correlation effects cause the shift of the sharp DOS peak away from the Fermi level and the obvious spin splitting around Fermi level in  $\text{Sm}_1\text{C}_{18}\text{H}_{12}$ . As a result, the electronic states at the Fermi level obviously decrease. However,  $\text{Sm}_1\text{C}_{18}\text{H}_{12}$  still exhibits the metallic feature when  $U = 5.5$  eV, which is different from Sm-doped phenanthrene where behaves as semiconductor with a small gap of 0.12 eV as  $U = 6$  eV.<sup>15</sup> To check our results, we have also calculated the total DOS of  $\text{Sm}_1\text{C}_{18}\text{H}_{12}$  at different  $U$  values, such as 6, 7, 8 and 9 eV. The results are shown in Fig. 3. We find that  $\text{Sm}_1\text{C}_{18}\text{H}_{12}$  is still metallic under different  $U$  parameters, and the electronic states near the Fermi level have the similar characteristics with the change of  $U$ . The results shows that the  $U = 5.5$  eV is efficient enough, and further verifies the metallicity of  $\text{Sm}_1\text{C}_{18}\text{H}_{12}$  different from Sm-doped phenanthrene.<sup>15</sup>

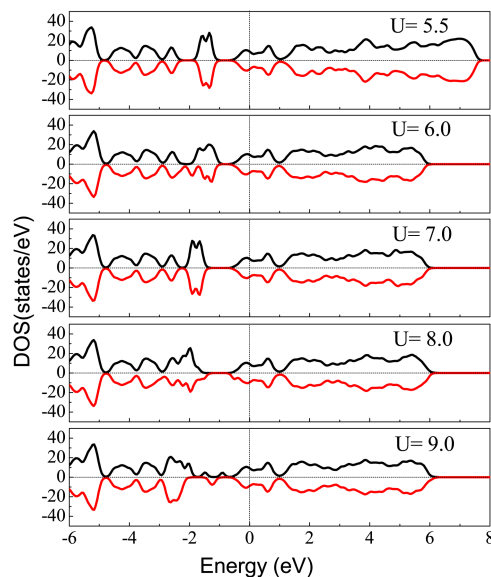


FIG. 3. Calculated total DOS of the most stable  $\text{Sm}_1\text{C}_{18}\text{H}_{12}$  based on the GGA+ $U$  method with different  $U$  values. Zero energy denotes the Fermi level.

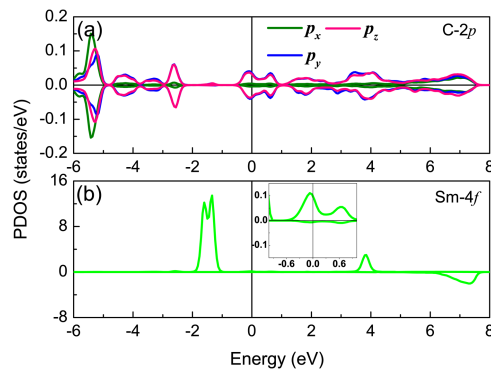


FIG. 4. Calculated PDOS onto the  $2p$  ( $p_x$ ,  $p_y$ , and  $p_z$ ) orbitals of C atom (a) and  $4f$  orbitals of Sm atom (b) of the most stable Sm-doped chrysene. The inset figure in (b) shows the PDOS of Sm- $4f$  atoms around the Fermi level (from -1 eV to 1 eV). Zero energy denotes the Fermi level.

The projected electronic DOS (PDOS) of a typical C atom and Sm atom obtained by GGA+ $U$  ( $U = 5.5$  eV) approach are shown in Fig. 4 for the most stable Sm-doped chrysene. We find that  $2p_y$  and  $2p_z$  of C atoms equally contribute to the electronic states near the Fermi level while the contribution of C- $2p_x$  can be ignored (See Fig. 4(a)). Under GGA+ $U$  method, Sm- $4f$  electronic states present apparent spin splitting and are localized below the Fermi level so that the minority-spin states are unoccupied as shown in Fig. 4(b). From the quantity of electronic states at the Fermi level, C- $2p$  and Sm- $4f$  has respectively the value of 1.5 states/eV and 0.1 states/eV around the Fermi level in Sm<sub>1</sub>C<sub>18</sub>H<sub>12</sub>. So C- $2p$  electrons mainly contribute to the electronic states around the Fermi level in Sm<sub>1</sub>C<sub>18</sub>H<sub>12</sub>, which is similar to that in K-doped PAH superconductors. However, the electronic correlation effects can not be ignored in Sm-doped chrysene. Additionally, The spin-up and spin-down band structures along the specified paths in the Brillouin zone are shown in Fig. 5. As DOS results discussed above, Sm<sub>1</sub>C<sub>18</sub>H<sub>12</sub> obviously exhibits the metallic feature both spin-up and spin-down channels. Interestingly, three bands cross the Fermi level in Sm<sub>1</sub>C<sub>18</sub>H<sub>12</sub> instead of two bands in K-doped picene and phenanthrene.<sup>17,20</sup> Our result indicates that Sm-doped chrysene has not only the similarity but also the particularity comparing with K-doped PAH superconductors. A further exhaustive study is imperative to understand the competing magnetic-superconductive mechanism of these rare-earth metal doped PAHs.

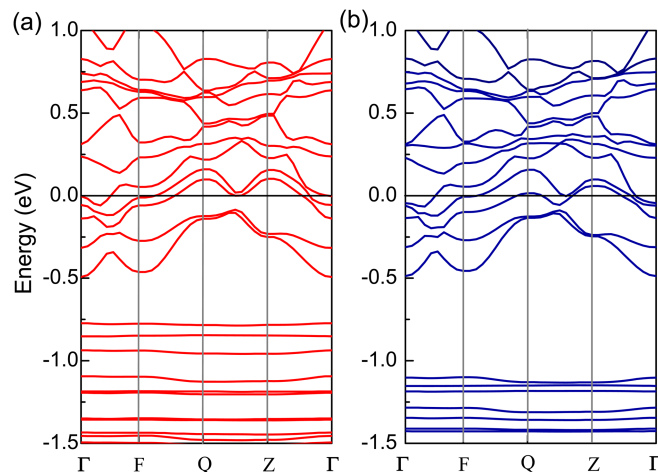


FIG. 5. Band structure of the most stable Sm<sub>1</sub>C<sub>18</sub>H<sub>12</sub>. (a) and (b) represent spin-up and spin-down electronic features respectively.

#### IV. CONCLUSIONS

In conclusion, we have investigated the crystal, magnetic characteristics and electronic structures of  $\text{Sm}_1\text{C}_{18}\text{H}_{12}$  by the first-principles calculation using GGA+ $U$  approach, also including vdW correction. With the help of full optimization, we found that Sm-doped chrysene with  $C2/c$  space group is the most stable, where doped Sm atoms stay on the relative middle of chrysene molecules. And for different magnetic configurations, it is indicated that Sm-doped chrysene is stabilized at the AFM ground-state with the metallic feature. The spin moment and orbital moment of Sm atom at the ground-state is respectively  $5.9 \mu_B$  and  $-1.6 \mu_B$ , which shows that two electrons are transferred from Sm to chrysene molecule in  $\text{Sm}_1\text{C}_{18}\text{H}_{12}$ . Within the framework of GGA+ $U$ , the electronic states around the Fermi level are mainly contributed by C- $2p$ , and three bands cross the Fermi level. The results indicate that the electronic correlation effects are not to be ignored to understand the superconductivity in  $\text{Sm}_1\text{C}_{18}\text{H}_{12}$  as well as other PAHs doped by rare-earth elements.

#### ACKNOWLEDGMENTS

The work was supported by the National Natural Science Foundation of China (no. 11274335) and the ITC funding of Shen Zhen (no. JCYJ20150521144320993). H. Q. Lin acknowledges support from NSFC U1530401 and computational resource from the Beijing Computational Science Research Center.

- <sup>1</sup> R. Mitsuhashi, Y. Suzuki, Y. Yamanari, H. Mitamura, T. Kambe, N. Ikeda, H. Okamoto, A. Fujiwara, M. Yamaji, N. Kawasaki, Y. Maniwa, and Y. Kubozono, *Nature (London)* **464**, 76 (2010).
- <sup>2</sup> X. F. Wang, R. H. Liu, Z. Gui, Y. L. Xie, Y. J. Yan, J. J. Ying, X. G. Luo, and X. H. Chen, *Nat. Commun.* **2**, 507 (2011).
- <sup>3</sup> Y. Kubozono, M. Mitamura, X. Lee, X. He, Y. Yamanari, Y. Takahashi, Y. Suzuki, Y. Kaji, R. Eguchi, K. Akaike, T. Kambe, H. Okamoto, A. Fujiwara, T. Kato, T. Kosugi, and H. Aoki, *Phys. Chem. Chem. Phys.* **13**, 16476 (2011).
- <sup>4</sup> M. Q. Xue, T. B. Cao, D. M. Wang, Y. Wu, H. X. Yang, X. L. Dong, J. B. He, F. W. Li, and G. F. Chen, *Sci. Rep.* **2**, 389 (2012).
- <sup>5</sup> X. F. Wang, X. G. Luo, J. J. Ying, Z. J. Xiang, S. L. Zhang, R. R. Zhang, Y. H. Zhang, Y. J. Yan, A. F. Wang, P. Cheng, G. J. Ye, and X. H. Chen, *J. Phys.: Condens. Matter* **24**, 345701 (2012).
- <sup>6</sup> G. A. Artioli, F. Hammerath, M. C. Mozzati, P. Carretta, F. Corana, B. Mannucci, S. Margadonna, and L. Malavasi, *Chem. Commun.* **51**, 1092 (2015).
- <sup>7</sup> J. P. Perdew, K. Burke, and M. Ernzerhof, *Phys. Rev. Lett.* **77**, 3865 (1996).
- <sup>8</sup> V. I. Anisimov, J. Zaanen, and O. K. Andersen, *Phys. Rev. B* **44**, 943 (1991).
- <sup>9</sup> A. I. Liechtenstein, V. I. Anisimov, and J. Zaanen, *Phys. Rev. B* **52**, R5467 (1995).
- <sup>10</sup> G. Kresse and J. Furthmüller, *Comput. Mater. Sci.* **6**, 15 (1996).
- <sup>11</sup> K. Lee, E. D. Murray, L. Kong, B. I. Lundqvist, and D. C. Langreth, *Phys. Rev. B* **82**, 081101 (2010).
- <sup>12</sup> G. H. Zhong, C. Zhang, X. W. Yan, X. G. Li, Z. Du, G. X. Jing, C. C. Ma, and C. L. Yang, "Structural and electronic properties of potassium-doped 1,2;8,9-dibenzopentacene superconductor: Comparing with doped [7]phenacenes," unpublished.
- <sup>13</sup> T. M. Krygowski, A. Ciesielski, B. Swirski, and P. Leszczynski, *Pol. J. Chem.* **68**, 2097 (1994).
- <sup>14</sup> J. F. Herbst, R. E. Watson, and J. W. Wilkins, *Phys. Rev. B* **17**, 3089 (1978).
- <sup>15</sup> X. W. Yan, Y. Wang, M. Gao, D. Ma, and Z. Huang, *J. Phys. Chem. C* **120**, 22565 (2016).
- <sup>16</sup> S. S. Naghavi and E. Tosatti, *Phys. Rev. B* **90**, 075143 (2014).
- <sup>17</sup> T. Kosugi, T. Miyake, S. Ishibashi, R. Arita, H. Aoki, and J. Phys., *Soc. Jpn.* **78**, 113704 (2009).
- <sup>18</sup> G. H. Zhong, C. Zhang, G. F. Wu, Z. B. Huang, X. J. Chen, and H. Q. Lin, *J. Appl. Phys.* **113**, 17E131 (2013).
- <sup>19</sup> G. H. Zhong, Z. B. Huang, and H. Q. Lin, *IEEE T. Magn.* **50**, 1700103 (2014).
- <sup>20</sup> P. L. de Andres, A. Guijarro, and J. A. Vergés, *Phys. Rev. B* **84**, 144501 (2011).